https://dx.doi.org/10.21577/0103-5053.20200236

J. Braz. Chem. Soc., Vol. 32, No. 4, 852-859, 2021
Printed in Brazil - ©2021 Sociedade Brasileira de Química

Article

[5]Helicene-Scaffold Fluorescence Sensing for Selective Detection of Au^{3+} Ions and Gold Nanoparticle

Pichayanun Sinthuprasert,[a] Anuwut Petdum,[b] Pattanawit Swanglap,[a] Waraporn Panchan,[b] Thanasat Sooksimuang,[b] Nantanit Wanichacheva[a] and Krit Setthakarn[,a]*

[a]*Department of Chemistry, Faculty of Science, Silpakorn University, 73000 Nakhon Pathom, Thailand*

[b]*National Metal and Materials Technology Center (MTEC), 12120 Pathumthani, Thailand*

A new quenching fluorescence sensor (MDP) with high productivity was easily synthesized from a [5]helicene anhydride derivative and propargyl bromide. This MDP sensor has significant photophysical properties, including high fluorescence emission and a large Stokes shift, and it exhibits selectivity and an excellent detection response in distinguishing Au^{3+} ions from interfering metal ions in aqueous solution. The limit of detection of the sensor were determined to be 0.16 μmol L^{-1} or 32.0 ppb. Stoichiometric binding between the MDP and Au^{3+} ions was found to occur at a 1:2 ratio. Additionally, the MDP sensor shows an ability to detect gold ions in real water samples and recognize gold nanoparticles (AuNPs), which invites its further application in biological and environmental systems.

Keywords: fluorescence sensor, [5]helicene, gold ions, gold nanoparticle

Introduction

Gold is a highly valued element in the world's economies and industries, being used as a catalyst in material production processes and as a commodity for the manufacture of coins, jewelry, and accessories. Gold is an abundant natural element that occurs in many forms.[1] One such form is the gold nanoparticle, which is a common and essential ingredient in cosmetics,[2] in the delivery of drug agents,[3-7] as a biomarker,[8-13] as a catalyst in industrial production processes,[14-17] and as a material for connecting elements in electronic chips.[18-21] The numerous uses of gold has led to the accumulation of hazardous wastes such as electronic waste[22] and gold-mining post-production waste,[23] which contain leftover gold and cause pollution and harm to living things. Although gold is biologically benign, in ion species it is very reactive and potentially noxious to humans. Gold ions can interact with human biomolecules, especially deoxyribonucleic acid (DNA) and proteins, which can damage the kidneys, liver, and peripheral nervous system.[24,25] Thus, it is important to develop methods for detecting gold ions in biological and environmental systems.

Ordinarily, gold ions are investigated using traditional methods, which involve complex reparation samples and the use of expensive and large instruments. Some methods employ chromatographic techniques, which have poor quantitative accuracy, including atomic absorption spectrometry (AAS),[26-28] inductively coupled plasma atomic emission spectrometry (ICP-AES),[29,30] and the electrochemical analysis method.[31,32] In contrast, fluorescence spectrometry is a better sensor technique for gold ions, given that it is low in cost, has high sensitivity and selectivity, and is convenient to perform.[1]

In recent years, research was conducted on a new five-ring helicene derivative,[33] which had a high fluorescence quantum yield and very large Stokes shifts. These exceptional optical properties include strong fluorescence emissions that promote the wide generation of organic light-emitting diodes and can be produced as a fluorophore for the analysis of various metal ions, although few studies have addressed this topic. Our research team has published two reports to date.[34,35] Herein, we present our design of a propargyl group as an ionophore for the detection and binding of Au^{3+}, which represents a significant advance in research on gold-detection sensors.[36,37] The fluorescence sensor (MDP) can be easily synthesized and developed as an effective sensor that has higher sensitivity and selectivity in the detection of Au^{3+} than other metal ions. The MDP sensor can detect Au^{3+} in an aqueous organic solution and real water sample. Additionally, this sensor can detect gold nanoparticles (AuNPs), which means it

*e-mail: krit.sett@gmail.com

can be used to detect gold in the environment and other systems.

Experimental

Materials and methods

All the chemicals used in this analysis study were purchased from the Fluka Chemical Corporation (Buchs, Switzerland) and Sigma-Aldrich Corporation (St. Louis, USA) and were used without further purification. A river water and sea water samples were collected from Mae Klong river and Don Hoi lot coast in Thailand, respectively. The ^{1}H and ^{13}C nuclear magnetic resonance (NMR) spectra were recorded on a nuclear magnetic resonance instrument at 300 MHz (Bruker 300). All UV-Vis absorption data were recorded by an Agilent-Cary 60 UV-Vis spectrophotometer. All fluorescence measurements were performed on a PerkinElmer Luminescence spectrometer model LS-50B in a quartz cuvette (1 × 1 cm) at a scan rate at 500 nm min^{-1} and a slit width of 5.0/5.0 nm. The excitation wavelength of the sensor was 373 nm and the emission spectra were within a range of 440-680 nm.

Synthesis

Synthesis of [5]helicene anhydride derivative (M202)

The [5]helicene anhydride derivative (M202) was prepared as described in a previous report.[38]

Synthesis of M202-EA (MEA)

M202 (100 mg, 0.26 mmol) was dissolved in *N*,*N*-dimethylformamide (DMF) (5 mL) in a 25-mL round bottom flask. Glacial acetic acid (0.5 mL, 8.7 mmol) and ethanolamine (0.18 mL, 2.98 mmol) were added to the stirred solution. The mixture was stirred in an argon atmosphere at 110 °C for 24 h. After cooling to room temperature, the crude product was extracted with EtOAc and washed with brine. The solvent was removed under reduced pressure. The crude product was purified by recrystallization using a mixture of EtOAc and hexane to yield MEA (103.4 mg, 94% yield) as a yellow solid; Rf 0.34 in CH_3OH:CH_2Cl_2 (1:20 v/v) as eluent; ^{1}H NMR (300 MHz, hexadeuterodimethyl sulfoxide (DMSO-d_6)) δ 2.28-2.33 (m, 2H, CH_2), 2.50 (s, 4H, CH_2), 2.76 (s, 2H, NCH_2), 3.57 (s, 2H, $C\underline{H_2}OH$), 3.90-3.94 (m, 2H, CH_2), 4.81 (t, 1H, *J* 5.6 Hz, $CH_2O\underline{H}$), 6.39 (d, 2H, *J* 8.5 Hz, 2Ar-H), 6.81 (s, 2H, 2Ar-H), 6.98 (d, 2H, *J* 9.5 Hz, 2Ar-H), 9.65 (s, 2H, 2Ar-OH); ^{13}C NMR (75 MHz, DMSO-d_6) δ 23.78, 28.13, 39.87, 58.01, 113.03, 114.12, 124.50, 124.58, 130.76, 136.80, 137.22, 140.71, 157.31, 168.31; HRMS (ESI) *m/z*, calcd. for $C_{26}H_{21}NO_5Na$ $[M + Na]^+$: 450.1312, found: 450.1310.

Synthesis of M202-DP (MDP)

MEA (50 mg, 0.1 mmol), K_2CO_3 (68.6 mg, 0.48 mmol), and propargyl bromide (0.18 mL, 2.4 mmol) were dissolved in acetone (3 mL) in a 10-mL round bottom flask. The reaction was refluxed in argon atmosphere for 48 h. After cooling to room temperature, the mixture product was extracted with CH_2Cl_2 and washed with brine (sat. aq. NaCl). The solvent was removed under reduced pressure. The crude product was purified by recrystallization using a mixture of CH_2Cl_2 and CH_3OH to yield MDP (42.5 mg, 72% yield) as a yellow solid; Rf 0.69 in CH_3OH:CH_2Cl_2 (1:20 v/v) as eluent; ^{1}H NMR (300 MHz, $CDCl_3$) δ 2.47-2.51 (m, 2H, CH_2), 2.55-2.60 (m, 2H, 2CH), 2.82-2.87 (m, 4H, $2CH_2$), 3.87 (s, 2H, NCH_2 and 2H, $C\underline{H_2}OH$), 4.02-4.07 (m, 2H, CH_2), 4.70 (s, 4H, $2OCH_2$), 6.57 (d, 2H, *J* 8.7 Hz, 2Ar-H), 6.70 (s, 2H, 2Ar-H), 7.15 (d, 2H, *J* 8.7 Hz, 2Ar-H); ^{13}C NMR (75 MHz, $CDCl_3$) δ 24.18, 28.98, 40.63, 55.77, 61.42, 75.80, 78.39, 112.64, 113.47, 125.23, 127.18, 131.14, 131.35, 138.04, 138.18, 141.03, 157.43, 169.53; HRMS (ESI) *m/z*, calcd. for $C_{32}H_{25}NO_5Na$ $[M + Na]^+$: 526.1625, found: 526.1624.

Results and Discussion

Design and syntheses

We investigated the helicene anhydride derivative (M202) for its use as a fluorophore in a fluorescent sensor due to its fluorescence behaviors, i.e., large Stokes shift and high fluorescence quantum yield. In addition, the propargyl group contains a terminal alkyne moiety that is selective and reactive to Au^{3+} ions for transforming the terminal alkyne into ketone via a hydration reaction. Therefore, M202 was connected with the propargyl moiety to serve as a new Au^{3+} fluorescence sensor (MDP). The MDP sensor was synthesized in two sequential steps: imidation and alkylation (Scheme 1). First, the imidation reaction of M202 and ethanolamine under acidic conditions provided an excellent yield of MEA. Then, we reacted MEA with propargyl bromide via alkylation to obtain a high yield of the MDP sensor. This MDP chemosensor comprises a [5]helicene component for fluorescence signaling and a terminal alkyne group that performs selective Au^{3+} ion recognition. The structures of MEA and MDP were successfully characterized and confirmed using ^{1}H NMR, ^{13}C NMR and mass spectroscopy (Figures S1-S8, Supplementary Information (SI) section).

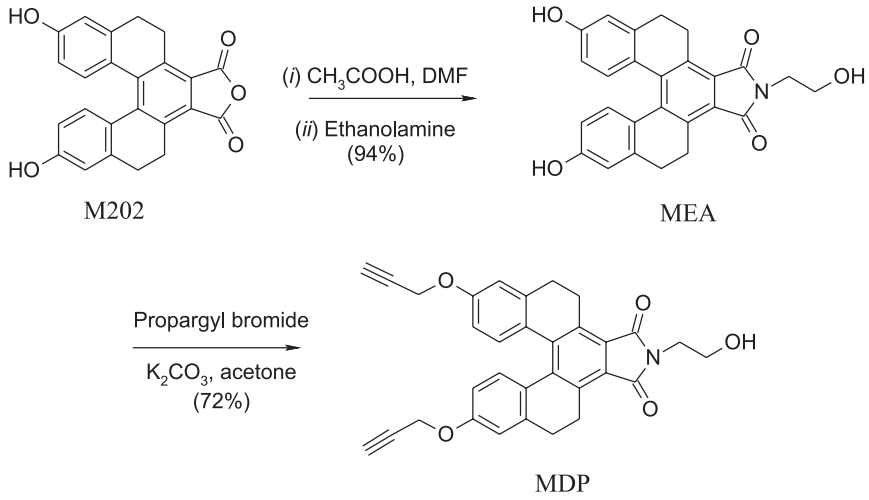

Scheme 1. Synthesis of MDP.

Optical properties

The optical properties of MDP were investigated before and after binding with Au^{3+} ions (MDP-Au^{3+}) by UV-Vis and fluorescence spectroscopies in aqueous solution (Figure 1). The UV-Vis absorption spectra of MDP ranged from 330-650 nm, with the λ_{max} value at 373 nm. Fluorescence emission signals were collected at 530 nm, with excitation wavelengths of 373 nm. A large Stokes shift obviously occurred at around 157 nm, which reduced the self-absorption phenomena of the MDP sensor. The excitation at 373 nm was chosen to study the change in the fluorescence emission signals of the MDP sensor with and without Au^{3+} ions, along with related experiments.

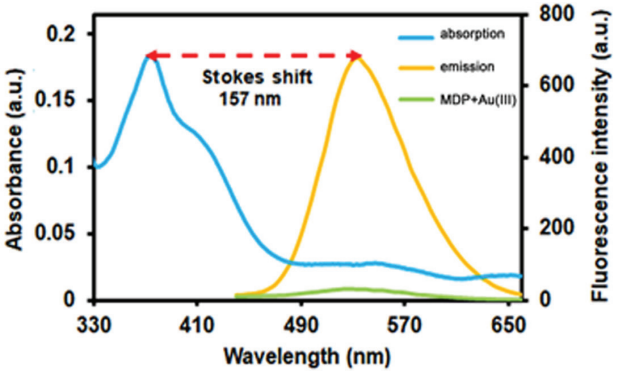

Figure 1. UV-Vis absorption and fluorescence spectra of MDP (1.5 μmol L^{-1}) in HEPES buffer solution (5 mmol L^{-1}, pH 7.2) and MDP-Au^{3+} (Au^{3+}: 20.0 μmol L^{-1}).

Sensitivity studies

The binding sensitivity was determined by UV-Vis and fluorescence titration of MDP with an Au^{3+} ion concentration range of 0-26.7 μmol L^{-1} in a 4-(2-hydroxyethyl)-1-piperazineethanesulfonic acid (HEPES) buffer solution (5 mmol L^{-1}, pH 7.2). For the UV-Vis titration studies (Figure S9, SI section), MDP exhibited decreasing of absorbance at 340-400 nm when the concentration of Au^{3+} in the solution was increased. In addition, the fluorescence measurement (Figure 2) revealed that MDP sensor showed a strong fluorescence at 530 nm in absence of Au^{3+}. However, when the sensor was treated with Au^{3+} ions, the fluorescence emission peak at 530 nm was significantly quenched. With the continuous titration of MDP with Au^{3+} ions, a linear relationship was identified by plotting the quenched fluorescence intensity against the concentration of added Au^{3+} ions, with the linear working range found to be 3-17 μmol L^{-1}. Additionally, the limit of detection of MDP was calculated to be 0.16 μmol L^{-1} or 32.0 ppb (Figure 3).

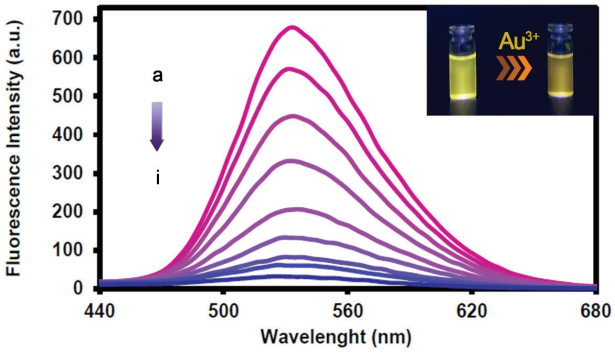

Figure 2. Fluorescence spectra of MDP (1.5 μmol L^{-1}) in HEPES buffer solution (5 mmol L^{-1}, pH 7.2) after titration with various concentrations of Au^{3+} (a) 0 μmol L^{-1}, (b) 3.3 μmol L^{-1}, (c) 6.7 μmol L^{-1}, (d) 10.0 μmol L^{-1}, (e) 13.3 μmol L^{-1}, (f) 16.7 μmol L^{-1}, (g) 20.0 μmol L^{-1}, (h) 23.3 μmol L^{-1}, (i) 26.67 μmol L^{-1}.

The limit of detection of the MDP was adequate for determining the exposure of contaminated Au^{3+} ions in an aqueous source, such as an ecosystem or industrial waste. The detection-time dependence of MDP was determined, the results show that the change in the fluorescence intensity

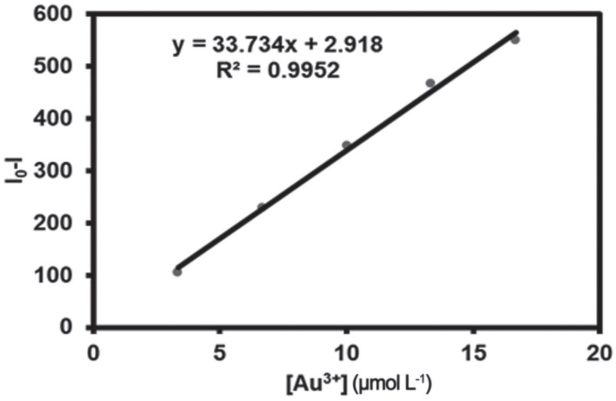

Figure 3. Linear correction of MDP (1.5 μmol L^{-1}) in HEPES buffer solution (5 mmol L^{-1}, pH 7.2) after titration with various concentrations of Au^{3+} (3-17 μmol L^{-1}) (S/N = 3).

remained constant within 30 min after titration with Au^{3+} ions. Moreover, the fluorescence quantum yield (Φ_f) of MDP was determined. The observed result was 0.2 which compared with 9,10-diphenylanthrancene as a reference standard. The sensing efficacy of MDP-Au^{3+} was equal to or more effective than other previously reported Au^{3+} sensors, as summarized in Table 1.

Binding study

To understand the complex mechanism of the MDP-Au^{3+} sensor, the Job plot was examined by fluorescence spectroscopy (Figure 4). The plot of the relative fluorescence intensities and mole fractions of the added Au^{3+} ions indicated that the mole ratio between MDP and Au^{3+} was 1:2, as shown in Figure 4. To determine the binding constant, we applied the Benesi-Hildebrand equation and determined the association constant (K_{assoc}) to be 1.92×10^{10} mol^2 L^{-2}.

Table 1. Comparison of sensing characteristics of reported Au^{3+} sensors and the sensor developed in this work

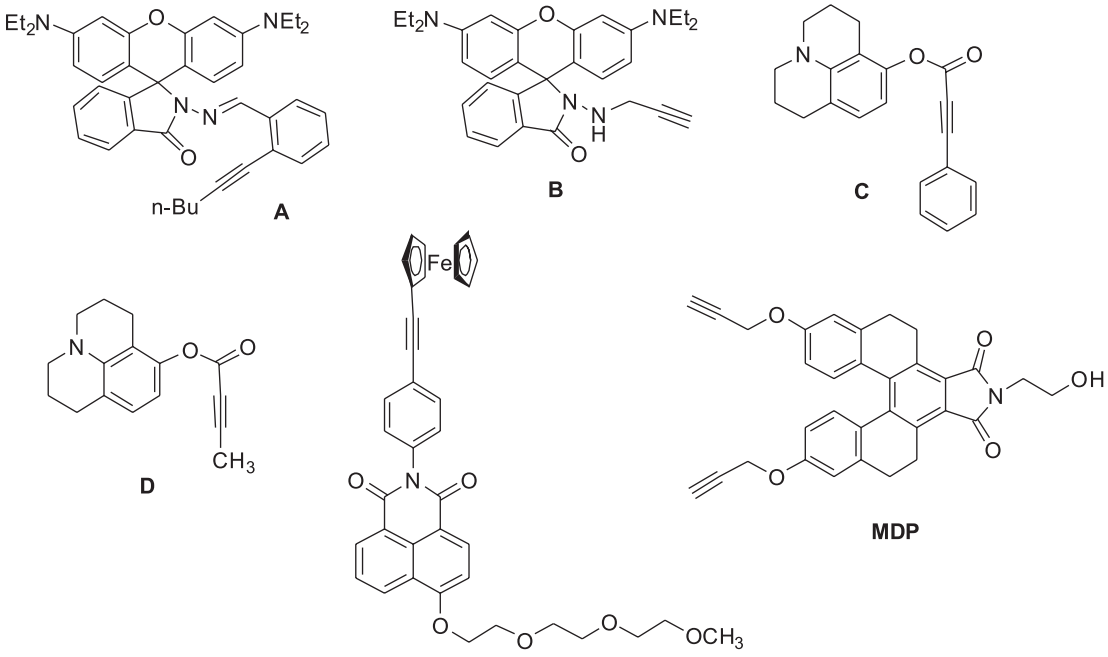

Compound	Sensitivity[a]	Stokes shift / nm	$\lambda_{ex}/\lambda_{em}$ / nm	Working system	Reference
A	0.6 ppm, 60 min	80	500/580	CH_3CN/HEPES buffer (1:1, v/v, pH 7.0)	39
B	36 ppb, 30 min	25	553/578	EtOH/PBS buffer (1:1, v/v, pH 7.4)	40
C	19.7 ppm	96	415/511	EtOH/HEPES buffer (1:1, v/v, pH 7.4)	41
D	23.6 ppm	67	400/467	EtOH/HEPES buffer (1:1, v/v, pH 7.4)	41
E	95 ppb, 15 min	84	369/453	CH_3CN/PBS buffer (1:1, v/v, pH 8.0)	42
MDP	32.0 ppb, 30 min	157	373/530	HEPES buffer (5 mmol L^{-1}, pH 7.2)	this work

[a]Limit of detection and response time. λ_{ex}: excitation wavelength; λ_{em}: emission wavelength; HEPES: 4-(2-hydroxyethyl)-1-piperazineethanesulfonic acid; PBS: phosphate buffered saline.

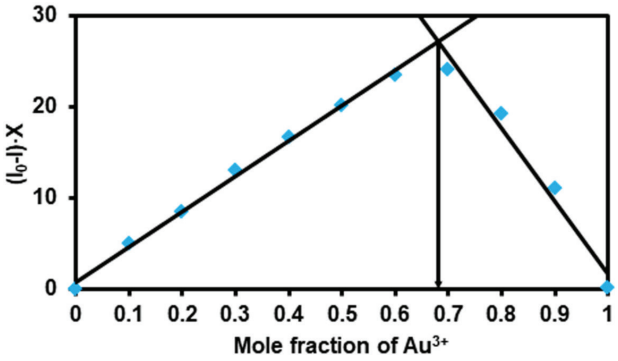

Figure 4. Job plot for MDP with Au^{3+} in HEPES buffer solution (5 mmol L^{-1}, pH 7.2) (S/N = 3).

pH effect study

To study the pH effect, MDP was titrated with Au^{3+} in a pH range of 3.0-10.0, the results were shown in Figure S10 (SI section). The fluorescence quenching was observed after the addition of Au^{3+} at all pH range. It could be noted that the sensor provided the remarkable fluorescence quenching toward Au^{3+} in acidic condition (pH < 5), which could adversely affect some analytical equipment. Moreover, the sensor also exhibited significant fluorescence quenching at pH ca. 7 (physiological pH) which was an environmentally friendly condition. Thus, pH 7.2 was selected as conditional parameter for Au^{3+}-sensing of the sensor.

Mechanistic study

To develop the sensing mechanism, the MDP sensor was reacted with a solution of Au^{3+} in acetonitrile.[43] The reaction mixture was then stirred at 40 °C for 48 h. The reaction was constantly observed by thin-layer chromatography (TLC), which indicated the quantity of MDP consumed during the reaction. However, the TLC results also indicated the formation of many products that had a variety of Rf values. Despite our best attempts, we were unable to isolate those products or characterize their structures by chromatographic techniques. Since the MDP contained Au^{3+}-reactive sites, i.e., propargyl groups on both sides, the most plausible Au^{3+}-detection mechanism is the mechanism described in previous studies by the Dong *et al.*[44] and Li *et al.*[45] groups.

To understand the reaction mechanism of MDP with Au^{3+}, the Fourier transform infrared with attenuated total reflectance (FTIR-ATR) spectra of MDP and MDP-Au^{3+} complex were explored. As can be seen in Figure S11, SI section, the FTIR-ATR spectra of MDP showed the strong transmittance at 1753 and 1692 cm^{-1} which correlated to C=O stretching of imide group, and the transmittance at 2120 cm^{-1} which correlated to alkyne of the propargyl groups of MDP. In contrast, the FTIR spectra of MDP-Au^{3+} complex not only exhibited the new transmission peak at 1642 cm^{-1}, which correlated to C=O stretching of the ketone-product, but the transmittance of alkyne (at 2120 cm^{-1}) also disappeared. Additionally, the transmission peaks of the imide group (1753 and 1695 cm^{-1}) were still observed, which could be implied that the imide group did not react with or bound to Au^{3+}. These results indicated that Au^{3+} reacted with the propargyl group of MDP through gold-catalyzed alkyne hydration,[44] which led to formation of the ketone groups that connected to the [5]helicene moiety (Scheme S1, SI section).

Selectivity study

The MDP sensor was found to be an excellent candidate for detecting Au^{3+} ions. Next, we conducted selectivity test of the sensor against interfering metal ions, including Au^{3+}, Ag^{+}, Hg^{2+}, Cu^{2+}, Ca^{2+}, Cd^{2+}, Pb^{2+}, Na^{+}, K^{+}, Fe^{2+}, Fe^{3+}, Ba^{2+}, Al^{3+}, Mn^{2+}, Li^{+}, Ni^{2+}, Mg^{2+}, Zn^{2+}, Co^{2+}, and Cr^{2+} as well as anions (S^{2-}, Cl^{-} and CN^{-}). Figures 5-7 show the results of the selectivity tests obtained by fluorescence spectroscopy with quantitative titration between the MDP sensor and metal ions. Without adding any metal ions to the MDP solution, a fluorescence signal was obviously detected. In the presence of Au^{3+} ions, the fluorogenic behavior of the MDP changed. With the addition of Au^{3+}, the fluorescence signal of MDP decreased with increases in the concentration of Au^{3+}. This fluorogenic change indicated the chemosensing properties of the MDP sensor with respect to Au^{3+}. Further titration of MDP with competitive ions showed insignificant changes in its fluorescence signals, which indicates that the MDP sensor was highly selective to Au^{3+} against other metal ions (Figures 7-8).

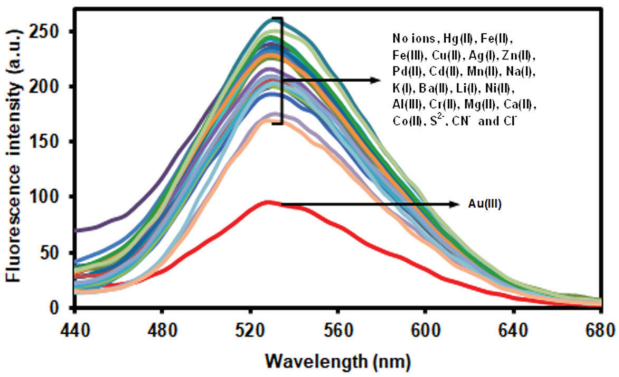

Figure 5. Fluorescence spectra (λ_{ex} = 373 nm) of MDP (1.5 μmol L^{-1}) in HEPES buffer solution (5 mmol L^{-1}, pH 7.2) with the addition of chloride salts of Au^{3+}, Ag^{+}, Hg^{2+}, Cu^{2+}, Ca^{2+}, Cd^{2+}, Pb^{2+}, Na^{+}, K^{+}, Fe^{2+}, Fe^{3+}, Ba^{2+}, Al^{3+}, Mn^{2+}, Li^{+}, Ni^{2+}, Mg^{2+}, Zn^{2+}, Co^{2+}, Cr^{2+}, S^{2-}, Cl^{-} and CN^{-} (15 μmol L^{-1}).

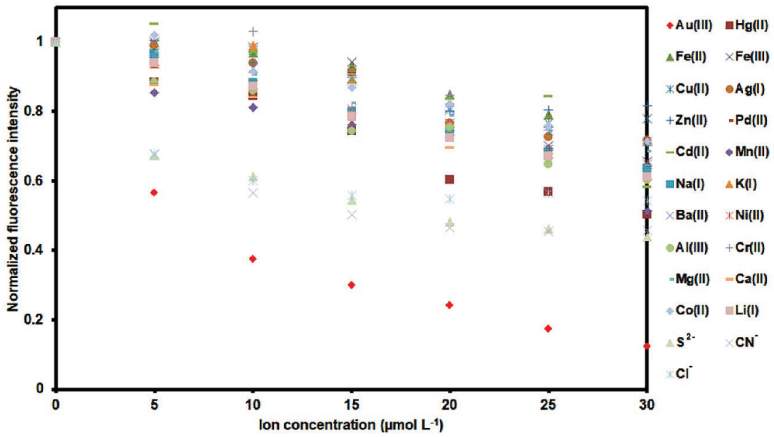

Figure 6. Normalized emission intensities (λ_{ex} = 373 nm) of MDP (1.5 μmol L^{-1}) in HEPES buffer solution (5 mmol L^{-1}, pH 7.2) with various concentrations of Au^{3+}, Ag^{+}, Hg^{2+}, Cu^{2+}, Ca^{2+}, Cd^{2+}, Pb^{2+}, Na^{+}, K^{+}, Fe^{2+}, Fe^{3+}, Ba^{2+}, Al^{3+}, Mn^{2+}, Li^{+}, Ni^{2+}, Mg^{2+}, Zn^{2+}, Co^{2+}, Cr^{2+}, S^{2-}, Cl^{-} and CN^{-}.

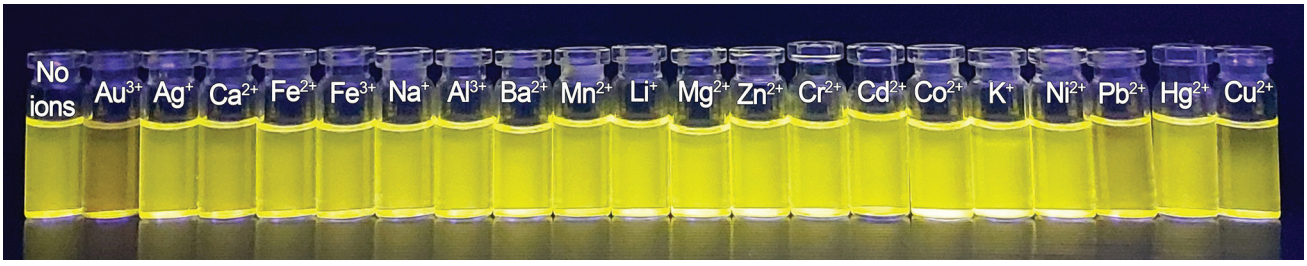

Figure 7. Fluorescence changes under UV light of MDP-Au^{3+} system with MDP (1.0×10^{-4} mol L^{-1}) and various metal ions (16.7 μmol L^{-1}): Au^{3+}, Ag^{+}, Hg^{2+}, Cu^{2+}, Ca^{2+}, Cd^{2+}, Pb^{2+}, Na^{+}, K^{+}, Fe^{2+}, Fe^{3+}, Ba^{2+}, Al^{3+}, Mn^{2+}, Li^{+}, Ni^{2+}, Mg^{2+}, Zn^{2+}, Co^{2+}, and Cr^{2+}.

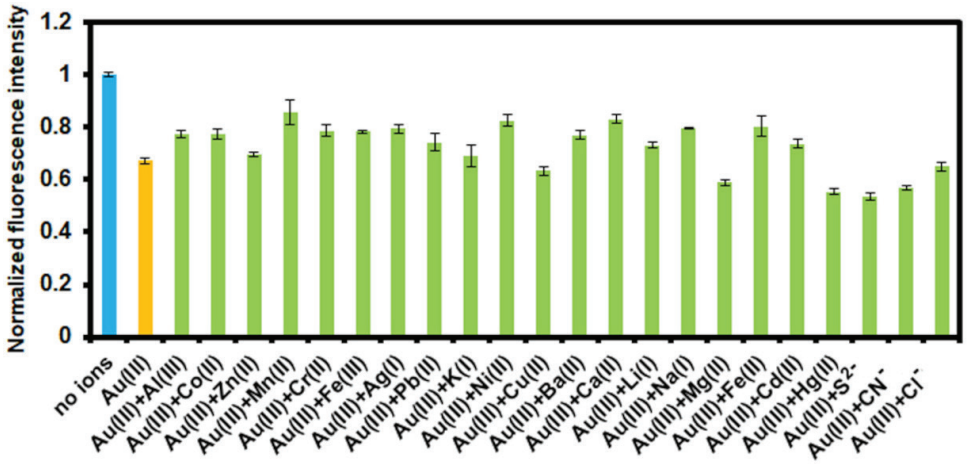

Figure 8. Competitive experiments with the MDP-Au^{3+} system with MDP (1.5 μmol L^{-1}) and various metal ions (15 μmol L^{-1}): Au^{3+}, Ag^{+}, Hg^{2+}, Cu^{2+}, Ca^{2+}, Cd^{2+}, Pb^{2+}, Na^{+}, K^{+}, Fe^{2+}, Fe^{3+}, Ba^{2+}, Al^{3+}, Mn^{2+}, Li^{+}, Ni^{2+}, Mg^{2+}, Zn^{2+}, Co^{2+}, Cr^{2+}, S^{2-}, Cl^{-} and CN^{-}.

Application of MDP for detecting Au^{3+} in real water samples

To study the ability of MDP for Au^{3+} detection in real water sample, fluorogenic change in river water (RW) and sea water (SW) were investigated after Au^{3+} were spiked (Figure 9). Both water samples, the emitting fluorescence of MDP decreased with Au^{3+} addition, therefore MDP could be used to recognize Au^{3+} in natural water.

Application of MDP for detecting gold nanoparticles (AuNPs)

Another application of the MDP sensor was investigated. Apart from Au^{3+} ions in aqueous solution, gold nanoparticles were used to further study the chemosensing properties of the MDP sensor. Gold nanoparticles were prepared according to Godwin's procedure.[46] The synthesized AuNPs was centrifuged at 10000 rpm to separate the supernatant. Then the AuNPs was rinsed by deionized water 3 times to remove

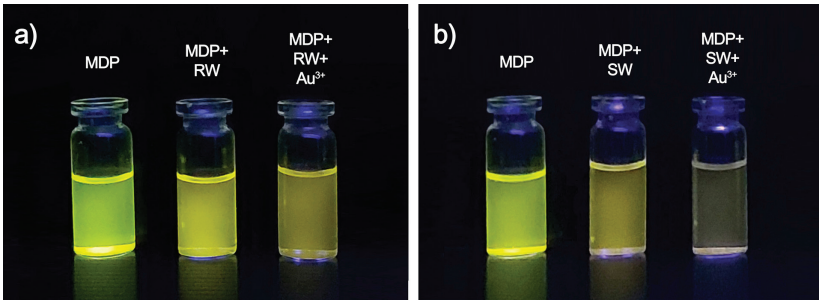

Figure 9. Fluorescence changes under UV light of MDP-Au^{3+} system with MDP (1.0×10^{-4} mol L^{-1}) and Au^{3+} (16.7 μmol L^{-1}) in (a) river water sample, (b) sea water sample.

excess reagents including Au^{3+}. Upon titrating MDP with a solution of gold nanoparticles, the emissions of the MDP sensor gradually lessened, much the same as by the addition of the Au^{3+} solution, as shown in Figure 10. The linear working range found to be 10-23 μmol L^{-1}. Moreover, the limit of detection was calculated to be 2.6 μmol L^{-1} or 0.51 ppm.

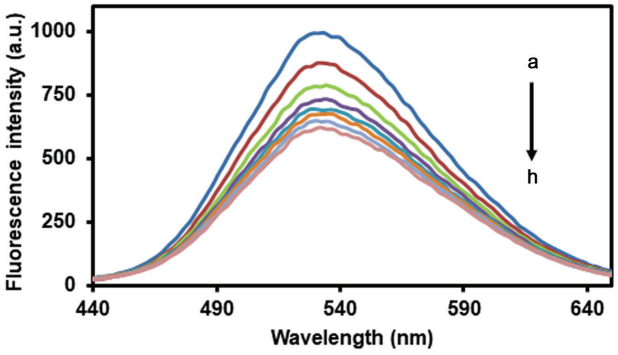

Figure 10. Fluorescence spectra of MDP (1.5 μmol L^{-1}) in HEPES buffer solution (5 mmol L^{-1}, pH 7.2) after titration with various concentrations of AuNPs (a) 0 μmol L^{-1}, (b) 3.3 μmol L^{-1}, (c) 6.7 μmol L^{-1}, (d) 10.0 μmol L^{-1}, (e) 13.3 μmol L^{-1}, (f) 16.7 μmol L^{-1}, (g) 20.0 μmol L^{-1}, (h) 23.3 μmol L^{-1}.

Conclusions

In summary, we developed a new fluorescence Au^{3+}-sensor (MDP) based on [5]helicene anhydride dye. The MDP sensor is synthesized in two convenient steps. The photophysical property of MDP was found to be a quenching signal, which is very sensitive and selective in detecting Au^{3+} ions in aqueous solution. The limit of detection of MDP for Au^{3+} was determined to be 0.16 μmol L^{-1} or 32.0 ppb, which could be used to determine the presence of contaminated or leftover Au^{3+} in natural sources and industrial wastes. We also tested MDP regarding its ability to detect gold nanoparticles in aqueous solution, which would also proved to be useful in future environmental applications.

Supplementary Information

Supplementary data are available free of charge at http://jbcs.sbq.org.br as PDF file.

Acknowledgments

Authors would like to thank grant RSA 6080058 from the Thailand Research Fund and Faculty of Science, Silpakorn University (grant SRIF-PRG-25634-01) for support this project.

Author Contributions

Pichayanun Sinthuprasert was responsible for data curation; Anuwut Petdum for data curation; Pattanawit Swanglap for data curation; Waraporn Panchan for data curation; Thanasat Sooksimuang for data curation; Nantanit Wanichacheva for conceptualization, data curation, funding acquisition, project administration, supervision, writing-review and editing; Krit Setthakarn for conceptualization, data curation, methodology, project administration, supervision, writing-original draft, writing-review and editing.

References

1. Singha, S.; Kim, D.; Seo, H.; Cho, S. W.; Ahn, K. H.; *Chem. Soc. Rev.* **2015**, *44*, 4367.
2. Cao, M.; Li, J.; Tang, J.; Chen, C.; Zhao, Y.; *Small* **2016**, *12*, 5488.
3. Salem, D. S.; Sliem, M. A.; El-Sesy, M.; Shouman, S. A.; Badr, Y.; *J. Photochem. Photobiol., B* **2018**, *182*, 92.
4. Yuan, X.; He, Y.; Zhou, G.; Li, X.; Feng, A.; Zheng, W.; *J. Photochem. Photobiol., B* **2018**, *183*, 147.
5. Ramírez-García, G.; Honorato-Colin, M. Á.; de la Rosa, E.; López-Luke, T.; Panikar, S. S.; de Jesús Ibarra-Sánchez, J.; Piazza, V.; *J. Photochem. Photobiol., A* **2019**, *384*, 112053.
6. Akram, M. W.; Raziq, F.; Fakhar-e-Alam, M.; Aziz, M. H.; Alimgeer, K.; Atif, M.; Amir, M.; Hanif, A.; Farooq, W. A.; *J. Photochem. Photobiol., A* **2019**, *384*, 112040.
7. Gholami, M.; Salmasi, M. A.; Sohouli, E.; Torabi, B.; Sohrabi, M. R.; Rahimi-Nasrabadi, M.; *J. Photochem. Photobiol., A* **2020**, 112523.

8. Grabowska, I.; Sharma, N.; Vasilescu, A.; Iancu, M.; Badea, G.; Boukherroub, R.; Ogale, S.; Szunerits, S.; *ACS Omega* **2018**, *3*, 12010.
9. Foguel, M. V.; dos Santos, G. P.; Ferreira, A. A. P.; Magnani, M.; Mascini, M.; Skladal, P.; Benedetti, A. V.; Yamanaka, H.; *J. Braz. Chem. Soc.* **2016**, *27*, 650.
10. Nordin, N.; Yusof, N. A.; Abdullah, J.; Radu, S.; Hajian, R.; *J. Braz. Chem. Soc.* **2016**, *27*, 1679.
11. Vidotti, M.; Carvalhal, R. F.; Mendes, R. K.; Ferreira, D. C. M.; Kubota, L. T.; *J. Braz. Chem. Soc.* **2011**, *22*, 3.
12. Li, M.; Wu, J.; Ma, M.; Feng, Z.; Mi, Z.; Rong, P.; Liu, D.; *Nanotheranostics* **2019**, *3*, 113.
13. Zhang, Z.; Liu, T.; Wang, S.; Ma, J.; Zhou, T.; Wang, F.; Wang, X.; Zhang, G.; *J. Photochem. Photobiol., A* **2019**, *370*, 89.
14. Hallett-Tapley, G. L.; Crites, C.-O. L.; González-Béjar, M.; McGilvray, K. L.; Netto-Ferreira, J. C.; Scaiano, J.; *J. Photochem. Photobiol., A* **2011**, *224*, 8.
15. Ciriminna, R.; Falletta, E.; Della Pina, C.; Teles, J. H.; Pagliaro, M.; *Angew. Chem., Int. Ed*. **2016**, *55*, 14210.
16. Silva, R. J. M.; Fiorio, J. L.; Vidinha, P.; Rossi, L. M.; *J. Braz. Chem. Soc.* **2019**, *30*, 2162.
17. Wojcieszak, R.; Cuccovia, I. M.; Silva, M. A.; Rossi, L. M.; *J. Mol. Catal. A: Chem.* **2016**, *422*, 35.
18. Luo, D.; Nakata, K.; Fujishima, A.; Liu, S.; *J. Photochem. Photobiol., C* **2017**, *31*, 139.
19. Fernandez, M.; Urvoas, A.; Even-Hernandez, P.; Burel, A.; Meriadec, C.; Artzner, F.; Bouceba, T.; Minard, P.; Dujardin, E.; Marchi, V.; *Nanoscale* **2020**, *12*, 4612.
20. Therézio, E. M.; Hidalgo, Á. A.; Oliveira Jr., O. N.; Silva, R. A.; Marletta, A.; *J. Braz. Chem. Soc.* **2015**, *26*, 1798.
21. Iliev, V.; Tomova, D.; Bilyarska, L.; *J. Photochem. Photobiol., A* **2018**, *351*, 69.
22. Yue, C.; Sun, H.; Liu, W. J.; Guan, B.; Deng, X.; Zhang, X.; Yang, P.; *Angew. Chem., Int. Ed*. **2017**, *56*, 9331.
23. Inoue, K.; Parajuli, D.; Gurung, M.; Pangeni, B.; Khunathai, K.; Ohto, K.; Kawakita, H. In *Element of Bioeconomy*; Biernat, K., ed.; IntechOpen: London, UK, 2019.
24. Wang, Y.; Liu, Y.; Miao, J.; Ren, M.; Guo, W.; Lv, X.; *Sens. Actuators, B* **2016**, *226*, 364.
25. Seo, H.; Jun, M. E.; Ranganathan, K.; Lee, K.-H.; Kim, K.-T.; Lim, W.; Rhee, Y. M.; Ahn, K. H.; *Org. Lett.* **2014**, *16*, 1374.
26. Özdemir, C.; Saçmacı, Ş.; Kartal, Ş.; Saçmacı, M.; *J. Ind. Eng. Chem.* **2014**, *20*, 4059.
27. Krawczyk, M.; Matusiewicz, H.; *J. Braz. Chem. Soc.* **2013**, *24*, 749.
28. Unsal, Y. E.; Tuzen, M.; Soylak, M.; *J. AOAC Int.* **2016**, *99*, 534.
29. Cellier, C.; Demoulin, O.; Salamone, C.; Navez, M.; Ruiz, P. In *Studies in Surface Science and Catalysis*, vol. 162; Gaigneaux, E. M.; Devillers, M.; de Vos, D. E.; Hermans, S.; Jacobs, P. A.; Martens, J. A.; Ruiz, P., eds.; Elsevier: London, UK, 2006.
30. Zhao, L.-C.; Wang, J.-G.; Li, X.; Zhang, S.; Zhang, Z.-F.; Hu, M.-Y.; Lu, F.; Wang, Y.-D.; Hu, Y.-Q.; Guo, X.-P.; Liu, Q.-X.; Liu, H.-J.; *Chin. J. Anal. Chem.* **2018**, *46*, e1801.
31. Kasper, A. C.; Veit, H. M.; García-Gabaldón, M.; Herranz, V. P.; *Electrochim. Acta* **2018**, *259*, 500.
32. Wu, Y.; Lai, R. Y.; *Anal. Chem.* **2016**, *88*, 2227.
33. Sahasithiwat, S.; Sooksimuang, T.; Kangkaew, L.; Panchan, W.; *Dyes Pigm.* **2017**, *136*, 754.
34. Petdum, A.; Panchan, W.; Swanglap, P.; Sirirak, J.; Sooksimuang, T.; Wanichacheva, N.; *Sens. Actuators, B* **2018**, *259*, 862.
35. Kaewnok, N.; Petdum, A.; Sirirak, J.; Charoenpanich, A.; Panchan, W.; Sahasithiwat, S.; Sooksimuang, T.; Wanichacheva, N.; *New J. Chem.* **2018**, *42*, 5540.
36. Li, Y.; Qiu, Y.; Zhang, J.; Zhu, X.; Zhu, B.; Liu, X.; Zhang, X.; Zhang, H.; *Biosens. Bioelectron.* **2016**, *83*, 334.
37. Wang, Q.; Feng, Y.; Jiang, J.; Wang, W.-J.; Chen, J.-Y.; Sheng, H.-T.; Meng, X.-M.; Zhu, M.-Z.; *Chin. Chem. Lett.* **2016**, *27*, 1563.
38. Jarutikorn, S.; Kraithong, S.; Sirirak, J.; Panchan, W.; Sooksimuang, T.; Charoenpanich, A.; *Orient. J. Chem.* **2019**, *35*, 1227.
39. Emrullahoğlu, M.; Karakuş, E.; Üçüncü, M.; *Analyst* **2013**, *138*, 3638.
40. Song, F.; Ning, H.; She, H.; Wang, J.; Peng, X.; *Sci. China: Chem.* **2014**, *57*, 1043.
41. Yang, Y.; Bai, B.; Jin, M.; Xu, Z.; Zhang, J.; Li, W.; Xu, W.; Wang, X.; Yin, C.; *Biosens. Bioelectron.* **2016**, *86*, 939.
42. Chinapang, P.; Ruangpornvisuti, V.; Sukwattanasinitt, M.; Rashatasakhon, P.; *Dyes Pigm.* **2015**, *112*, 236.
43. Wechakorn, K.; Prabpai, S.; Suksen, K.; Piyachaturawat, P.; Kongsaeree, P.; *RSC Adv.* **2016**, *6*, 24752.
44. Dong, M.; Wang, Y.-W.; Peng, Y.; *Org. Lett.* **2010**, *12*, 5310.
45. Li, Z.; Xu, Y.; Fu, J.; Zhu, H.; Qian, Y.; *Chem. Commun.* **2018**, *54*, 888.
46. McFarland, A. D.; Haynes, C. L.; Mirkin, C. A.; van Duyne, R. P.; Godwin, H. A.; *J. Chem. Educ.* **2004**, *81*, 544A.

Submitted: August 28, 2020
Published online: December 2, 2020